33rd Annual International Conference of the IEEE EMBS
Boston, Massachusetts USA, August 30 - September 3, 2011

A MRI-based platform for catheter navigation

Manuel Vonthron, *Student Member, IEEE*, Viviane Lalande, *Student Member, IEEE*
and Sylvain Martel, *Senior Member, IEEE*

Abstract— **The development of minimally invasive surgical techniques using magnetism is expanding. Our research group is exploring catheter steering using the gradient field of a modified clinical Magnetic Resonance Imaging (MRI) system. This paper focuses on the upgrade of the MRI testing platform towards an integrated system allowing for *in vitro* and *in vivo* experiments. The expected steering capabilities of the platform are evaluated through experimental tests, and catheter tracking is adapted accordingly while being tested for potential medical interventions.**

I. Introduction

External catheter actuation is a minimally invasive surgery technique that can be achieved by mechanical or magnetic means. Mechanical techniques such as the pull wire method [1], to name but only one technique, are hard to miniaturize due to the manufacturing and integration complexities preventing sufficient miniaturization of the instrument for medical interventions. The use of magnets at the tip of the catheter being actuated by external magnets [2] offers a solution to the miniaturization issue. The solution is pushed further by taking advantage of the dynamic magnetic properties of a Magnetic Resonance Imaging (MRI) system to steer devices such as catheters. The possibilities offered by this approach are numerous: this is not only about facilitating access to areas of the body currently difficult to operate on without causing damages, but also to allow treating areas that are inaccessible today with the promises of using a radiation-free imagery and steering capability.

Significant deformations are mandatory to distinguish the benefit brought by the magnetic steering from the surgeon's skills to navigate the catheter into tortuous vessel networks. The steering tests of a magnetic catheter tip using solely the gradient capacity of a clinical MRI system resulted into small tip displacements [3]. The same type of tests but with additional gradient coils inside the MRI system combined with an enhanced catheter tip design increased the force applied at the tip and showed wider deformations [4].

The "Magnetic Resonance Submarine" (MR-Sub) project aims at providing an integrated system capable of driving a device inside the human vascular system. Its approach is to use magnetic gradient force for microrobots-assisted medicine which is only one among the numerous research ways being listed in [5]. The final platform is intended to drive in fully autonomous or surgeon-guided way, a variety of devices including catheters [4] and synthetic microcarriers [6]. Every step involved, from device tracking to actual propulsion has been successfully validated *in-vivo* [7]. The experiments focused on a 2D steering of a 1.5mm diameter sphere in a permanent magnetic field $\overrightarrow{B_0}$. The magnetic force induced on the device by a magnetic gradient $\overrightarrow{\nabla B}$ can be estimated as

$$\vec{F}_{mag} = RV_m \cdot (\vec{M} \cdot \vec{\nabla})\vec{B} \quad (1)$$

where V_m is the volume of the ferromagnetic device (m^3), M its magnetization (A/m), and R the duty cycle, the time when magnetic gradients are applied within a cycle A clinical MRI system usually provides gradient $\overrightarrow{\nabla B}$ from 10 to 60 milliTesla per meter (mT/m) [8]. However, as mentioned in [9], the magnetic force from Eq.1 produced by such gradients cannot steer properly a sub-millimeter device since the force is proportional to the cube of the spherical device's diameter. Moreover, the imaging gradient coils of a clinical apparatus and their associated power-supply cannot experience a duty cycle higher than 50% at full amplitude [10]. On a Siemens Sonata MRI system for instance, this leads to an effective gradient amplitude of 20mT/m. We intend to drive sub-millimeter catheter tips and even smaller micro-devices. Thus, higher magnetic gradient amplitudes in the order of several hundreds mT/m [10], well beyond the capability of regular scanners, are required.

The new platform we present here offers gradient coils capabilities of more than 450 mT/m in the three directions of space (Fig. 1). They also can be combined for even better efficiency. We designed a whole hardware and software platform able to fulfill the goals of the MR-Sub project while not requiring any change to a standard clinical MRI scanner which makes it manufacturer-independent and model-independent as well. The platform could even be used while the MRI system is switched off. The discussed initial design is intended to be tested on a Siemens Sonata 1.5T MRI system.

II. System components

To achieve the goal of steering catheters, microparticles and other devices, the new two sets of coils are added as a complement of the existing equipment: A first one for steering purpose and a second one to provide imaging capabilities. Radiofrequency system of the MRI has to be re-done to image again through these new coils. A software

Manuscript received April 14, 2011. This project is supported in part by the Canada Research Chair (CRC) in Micro/Nanosystem Development, Fabrication and Validation and grants from the National Sciences and Engineering Research Council of Canada (NSERC), the Province of Québec, and the Canada Foundation for Innovation (CFI).
Manuel Vonthron (manuel.vonthron@polymtl.ca) and Viviane Lalande (viviane.lalande@polymtl.ca) are with the NanoRobotics laboratory, École Polytechnique de Montréal.
Corresponding author: Sylvain Martel, NanoRobotics Laboratory, École Polytechnique de Montréal, 2500 chemin de Polytechnique, Montréal (QC), Canada, H3T 1J4. (E-mail: sylvain.martel@polymtl.ca)

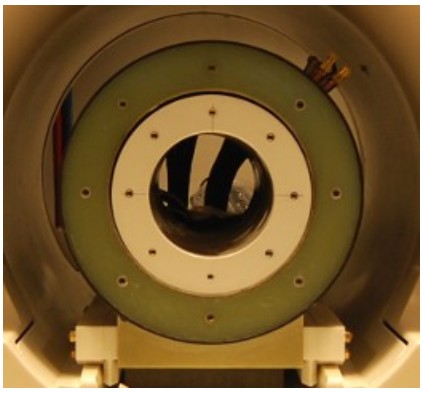

Fig. 1. Magnetic gradient coil sets inside the bore of a 1.5T Siemens Sonata MRI system – The outer cylinder is responsible of high amplitude and duty cycle gradients for propulsion. The inner cylinder provides high linearity and responsiveness gradients for imaging purpose.

architecture is also built to synchronize all components and control the propulsion with high precision.

A. Propulsion system

We mentioned that gradient amplitude of a clinical MRI system is not appropriate to bend enough a catheter to profit from the system nor drive sub-millimeter microparticles in presence of blood flow.

The new actuation system (Fig. 1) is made of a 400mm outer diameter cylinder embedding three pairs of magnetic gradient coils. A pair of longitudinal coils generates the *z*-axis gradient up to 510mT/m. Two pairs of transversal coils provide *x* and *y*-axis gradients, up to 460mT/m. Appropriate power supply and cooling allows a 100% duty cycle. The counterpart of these characteristics is a low slew rate and a minimum rise time of the coils and amplifier of 20ms. Long rise time are acceptable for propulsion stage but cannot allow imaging stages with this equipment. The propulsion coil set has been designed to maximize the magnetic force on the microdevice. It cannot be used as medical imaging equipment since its ramp up time and gradient uniformity are under medical imaging requirements.

B. Imaging and tracking system

Imaging and tracking coil set (Fig.1) reproduces the imaging capacity of the MRI system yet with higher imaging gradients amplitude. It is composed of the imaging set of coil and its associated amplification unit. The low-level control of both coils and the radio-frequency chain, i.e. the MRI sequence player, is provided by a versatile NMR spectrometer console. The positioning method of this new platform design is based on [11]. We implement it in the framework of the NMR spectrometer. The main characteristics of the coils is the ability to have very small rise time, down to 100µs, providing MRI quality images. While imaging pulse sequences usually do not need gradient amplitude higher than a few mT/m, these can also reach 500mT/m. The use of stronger gradient amplitude allows shortening the duration of the pulse and increasing the tracking rate.

C. Software architecture

The use of microrobot being propelled or a catheter being deflected at vessel bifurcations during minimally invasive surgery requires that the system is built upon highly reliable pieces of software. The architecture involves synchronization and communication between heterogeneous equipments. We choose to run a central controller computer running a hard real-time operating system (RTOS): Xenomai. This RTOS provides many programming facilities such as good hardware support, message passing framework, and real-time interface drivers. Also, the framework allows us to develop hard real-time applications in both kernel-space and user-space. Xenomai comes with the Analogy framework that we use to interface our controlling station with non-serial and non-network communication link such as TTL lines for synchronization or analog sampling for further evolutions that may include electrocardiograph (ECG) and other physiological sensors.

The main computer manages the heterogeneous equipments and runs the low level controller. The three systems run in a time-multiplexed fashion. Once the tracking pulse sequence is completed, the resulting raw RF data are sent to the controller which computes the correlation with the previous acquisition. It then computes the movement of the device (such as the catheter tip) [11] and generates appropriate propulsion or deflection orders depending on the types of devices being actuated. This results immediately following an accurate actuation of the device. Tracking and propulsion or deflection components in case of a catheter represent the environment of the real-time scheduling role played by the controller.

III. Preliminary Experiments

A. Propulsion measurements

In order to validate the possibility for catheter deflection while providing insights for the propulsion capabilities of the platform for untethered microrobots or carriers, we aimed to compare previous established experiments [4] with our new set of coils. The same boundaries conditions were applied in the previous and the new platform to guarantee that the data gathered would be related to the coils only. We reproduced the experiment with the custom Maxwell coils previously used along the *z*-axis and compared the results obtained with the ones from the new set of coils.

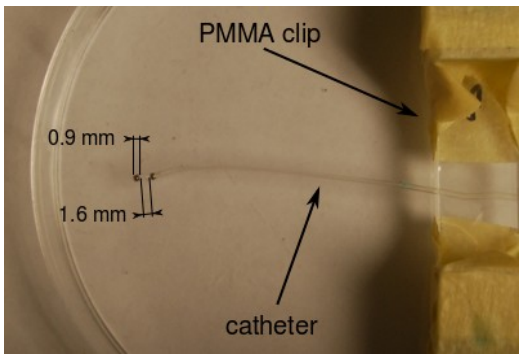

Fig. 2. Distal tip of the catheter with two 0.9mm chrome steel beads.

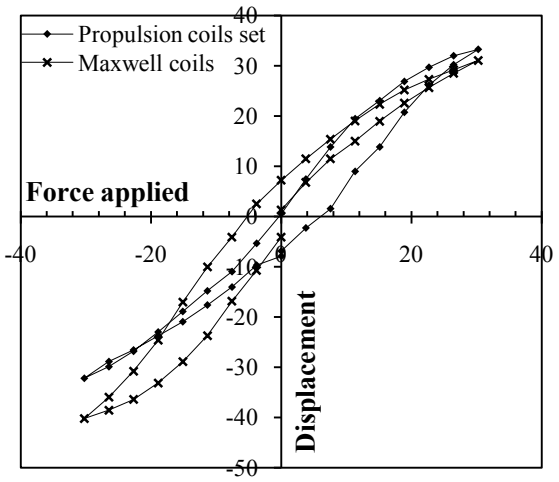

Fig. 3. Graph showing the displacement of the catheter versus the gradient amplitude inside the propulsion coil set and the Maxwell coils.

1) Material and method: A 2.5Fr catheter ("FasTracker 018", Boston Scientific, USA. (Fig. 2) of a 1.2×10^{-6} N.m^2 bending stiffness is clamped at 42mm from its distal tip. The tip of the catheter is composed of two chrome steel beads (Salemball, USA) spaced one from another with a hand-made PMMA spacer 1,6mm long in order to avoid an inconvenient torque described in [4]. The clamp and catheter are placed in a water bath to reduce friction. Each bead is 0.9mm diameter and has a 1 248 kA/m saturation magnetization. During both experiments, the gradient generated varies from -400 mT/m and +400 mT/m by steps of 50 mT/m. The displacement of the catheter relatively to its natural position when no gradient field is applied is measured at each step with a MRI compatible camera.

The setup is first placed between a pair of Maxwell coils (Fig 4(a)) and in the bore of a 1.5T Siemens Sonata MRI system so that the beads reach their saturation magnetization. The Maxwell coils are powered in order to produce a gradient field along the *z* axis of the MRI system.

The same setup is then placed at the center of the propulsion coil cylinder described in II-A inside the bore of the MRI system. This is depicted on Fig. 5(a). The free end of the catheter is placed in the homogeneity sphere of the coils set perpendicularly to the *z* axis. The whole experiment is repeated three times.

2) Results: Figure 4(b) and 5(b) show superimposed photographs of the deflections of the catheter inside the Maxwell coils and the propulsion coil set respectively. Each photograph represents a 50mT/m increment. Maximum amplitude and minimum amplitude correspond to our top values of 400 and -400mT/m. The comparison of the two pictures shows a highly similar behavior of the catheter regardless of the coil used and the repetition of the experiment. Considering that the displacement of displacement of the catheter highly depends on its stiffness and its free length, Figure 3 represents non-dimensional data of the displacement l of the catheter relatively to the force applied f for both systems. The applied force and the displacement are defined as :

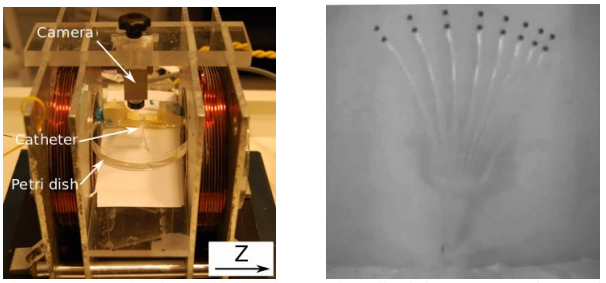

Fig. 4. Reproduction of experiment described in [1]: (a) shows the experimental setup; (b) is a superimposed picture of the deflections obtained by varying the gradient amplitude by 50mT/m increments from -400mT/m to +400mT/m.

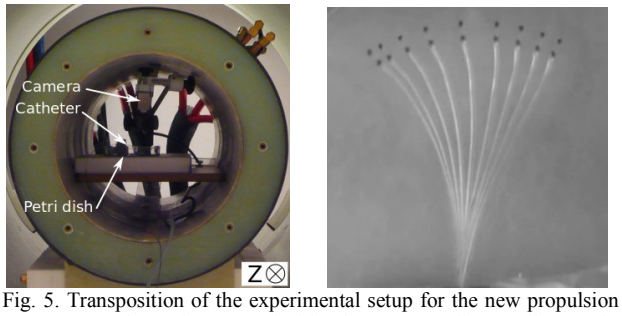

Fig. 5. Transposition of the experimental setup for the new propulsion system: (a) show the setup inside the new gradient coil set; (b) represents the superimposed pictures of deflections obtained by varying the gradient amplitude by 50mT/m increments from -400mT/m to +400mT/m along the *z* axis.

$$\vec{f} = \frac{\overrightarrow{F_{mag}}L^2}{EI}; \qquad l = \frac{d}{L} \tag{2}$$

Where f is the non-dimensional force applied, F_{mag} is the magnetic force (N) defined in Eq. 1, L is the length of the catheter from the clamp to the center of the first bead (m), EI is the measured stiffness of the catheter (N.m²), l is the non-dimensional displacement and d is the displacement of the tip of the catheter (m).

They both experience a hysteresis loop corresponding to the ferromagnetic behavior under a varying magnetic field. The two curves show a good correlation that validates the ability of the new coils to generate a magnetic force with the expected amplitude.

B. Tracking measurements

As the complete tracking set is not yet assembled, we first need to validate the tracking method with a clinical MRI system on the same type of catheter tip used in the first experiment. This measurement is achieved independently from the propulsion test.

1) Material and method: A one-bead tip catheter is manually moved inside a glass phantom mimicking a blood vessel in order to track the bead in *in-vitro* conditions. The phantom depicted on Fig. 6 is placed on a plastic stand used to lift it at the center of the MRI system's imaging zone. The phantom has a 2.8mm internal diameter and is 135mm long. The setup is immersed into a filled spherical aquarium to make sure that the catheter tip is surrounded with a large quantity of hydrogen protons for tracking requirements. The catheter is manually moved inside the glass phantom from one end to the other.

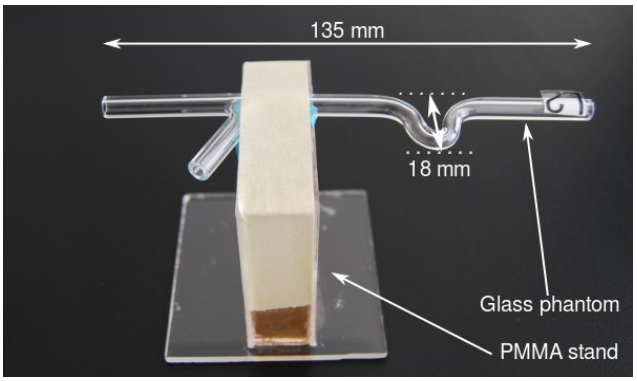

Fig. 6. Glass phantom mimicking curve and bifurcation of a blood vessel

A tracking MRI sequence is run during the actuation of the catheter. The sequence is tuned to best detect the displacement of the tip's bead by adjusting the excitation and acquisition frequency. The appropriate frequency offset is found by trial and errors. As soon as a displacement is computed, its coordinates are written in a text file. We perform a registration step on the collected data from the tracking program to match the coordinate origin. The points (X, Z) are then loaded as a "fiducial list" in the medical imaging visualization and computing software 3DSlicer.

2) Results: Figure 7 is a view of the 3DSlicer software very similar to what we propose to offer to the medical team during an operation. The image taken at the beginning of the procedure (path planning) is used as a background image to the points visualization. In this experiment we ran a regular HASTE imaging sequence on the model. The combination of the image and the tracked points shows that the trajectory is tracked as expected. Variations on the *x*-axis while the catheter is moved forward can be explained by the movement of the 0.9mm diameter tip inside the 2.9mm diameter tube and/or the tracking errors of the test. Maximum amplitude of this variation is up to 3.2mm. Considering the inner diameter of the model, this remains an acceptable precision to enable a closed-loop control on this basis.

IV. Discussion and Conclusion

The abilities of our new set of coils have been tested and they successfully provided the magnetic force needed to bend a catheter as expected and the tracking sequence has successfully been achieved on a catheter as well. Many tasks remain to be completed and the whole new platform with related critical components would need further tests and validations. The new set of coils proved their ability to bend a catheter and future work will focus on characterizing the catheter steering behavior and limitations with larger sample size of tests.

Therefore, future work will focus on the transfer of the tracking techniques developed on the MRI system to our new set of imaging coils. The synchronized activation of the propulsion and tracking elements through the main controller will be thoroughly tested.

Acknowledgment

The authors wish to acknowledge the support of the Nanorobotic Laboratory of Ecole Polytechnique de Montréal and particularly Frederick Gosselin, Gaël Bringout and Charles Tremblay.

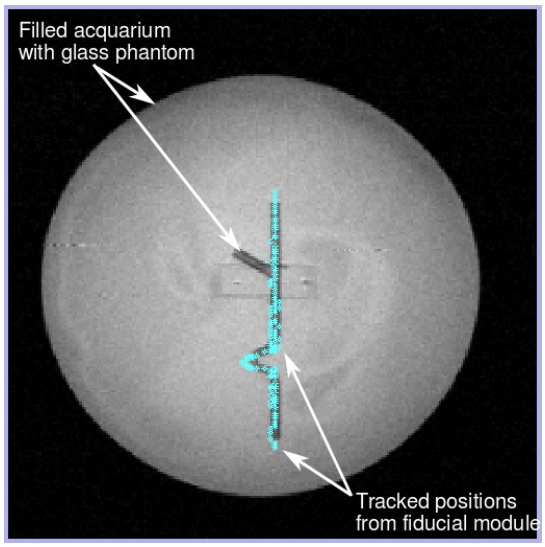

Fig. 7. Result of the catheter tracking in a glass phantom in a spheric aquarium. The dots represent the catheter tracked points as viewed in the fiducials module of 3DSlicer (medical imaging software).

References

[1] A. Al-Ahmad, J.D. Grossman, and P.J. Wang, "Early experience with a computerized robotically controlled catheter system," *Journal of interventional cardiac electrophysiology*, vol. 12, (no. 3), pp. 199-202, 2005.

[2] S. Ramcharitar, M. Patterson, R. van Geuns, C. van Meighem, and P. Serruys, "Technology insight: magnetic navigation in coronary interventions," *Nature Clinical Practice Cardiovascular Medicine*, vol. 5, (no. 3), pp. 148-156, 2008.

[3] K. Zhang, A. Krafft, R. Umathum, F. Maier, W. Semmler, and M. Bock, "Real-time MR navigation and localization of an intravascular catheter with ferromagnetic components," *Magnetic Resonance Materials in Physics, Biology and Medicine*, pp. 1–11.

[4] F. Gosselin, V. Lalande, and S. Martel, "Characterisation of the deflections of a catheter steered using a magnetic resonance imaging system," manuscript submitted for publication

[5] B. J. Nelson, I. K. Kaliakatsos, and J. J. Abbott, "Microrobots for minimally invasive medicine," *Annual Review of Biomedical Engineering*, vol. 12, pp. 55–85, June 2010.

[6] P. Pouponneau, O. Savadogo, T. Napporn *et al*., "Corrosion study of iron-cobalt alloys for MRI-based propulsion embedded in untethered microdevices operating in the vascular network*," Journal of Biomedical Materials Research Part B: Applied Biomaterials*, vol. 93, no. 1, pp. 203–211, 2010.

[7] J. Mathieu and S. Martel, "In vivo validation of a propulsion method for untethered medical microrobots using a clinical magnetic reso¬nance imaging system," in *Proceedings of the IEEE/RSJ International Conference on Intelligent Robots and Systems (IROS)*, San Diego, CA, 2007.

[8] C. Westbrook, C. Roth, and J. Talbot, *MRI in Practice*. Wiley-Blackwell, 2005.

[9] K. Belharet, D. Folio, and A. Ferreira, "MRI-based microrobotic system for the propulsion and navigation of ferromagnetic microcap-sules," *Minimally Invasive Therapy & Allied Technologies*, vol. 19, no. 3, pp. 157–169, 2010.

[10] J. Mathieu and S. Martel, "Steering of aggregating magnetic microparticles using propulsion gradients coils in an MRI Scanner," *Magnetic Resonance in Medicine*, vol. 63, no. 5, pp. 1336–1345, 2010.

[11] O. Felfoul, J. Mathieu, G. Beaudoin, and S. Martel, "In Vivo MR-Tracking Based on Magnetic Signature Selective Excitation," *IEEE Transactions on Medical Imaging*, vol. 27, no. 1, pp. 28–35, 2008.